

# Measurement of the Branching Fraction of $J/\psi \rightarrow \pi^+\pi^-\pi^0$

J. Z. Bai<sup>1</sup>, Y. Ban<sup>10</sup>, J. G. Bian<sup>1</sup>, X. Cai<sup>1</sup>, J. F. Chang<sup>1</sup>, H. F. Chen<sup>16</sup>, H. S. Chen<sup>1</sup>, H. X. Chen<sup>1</sup>, J. Chen<sup>1</sup>, J. C. Chen<sup>1</sup>, Jun Chen<sup>6</sup>, M. L. Chen<sup>1</sup>, Y. B. Chen<sup>1</sup>, S. P. Chi<sup>2</sup>, Y. P. Chu<sup>1</sup>, X. Z. Cui<sup>1</sup>, H. L. Dai<sup>1</sup>, Y. S. Dai<sup>18</sup>, Z. Y. Deng<sup>1</sup>, L. Y. Dong<sup>1</sup>, S. X. Du<sup>1</sup>, Z. Z. Du<sup>1</sup>, J. Fang<sup>1</sup>, S. S. Fang<sup>2</sup>, C. D. Fu<sup>1</sup>, H. Y. Fu<sup>1</sup>, L. P. Fu<sup>6</sup>, C. S. Gao<sup>1</sup>, M. L. Gao<sup>1</sup>, Y. N. Gao<sup>14</sup>, M. Y. Gong<sup>1</sup>, W. X. Gong<sup>1</sup>, S. D. Gu<sup>1</sup>, Y. N. Guo<sup>1</sup>, Y. Q. Guo<sup>1</sup>, Z. J. Guo<sup>15</sup>, S. W. Han<sup>1</sup>, F. A. Harris<sup>15</sup>, J. He<sup>1</sup>, K. L. He<sup>1</sup>, M. He<sup>11</sup>, X. He<sup>1</sup>, Y. K. Heng<sup>1</sup>, H. M. Hu<sup>1</sup>, T. Hu<sup>1</sup>, G. S. Huang<sup>1</sup>, L. Huang<sup>6</sup>, X. P. Huang<sup>1</sup>, X. B. Ji<sup>1</sup>, Q. Y. Jia<sup>10</sup>, C. H. Jiang<sup>1</sup>, X. S. Jiang<sup>1</sup>, D. P. Jin<sup>1</sup>, S. Jin<sup>1</sup>, Y. Jin<sup>1</sup>, Y. F. Lai<sup>1</sup>, F. Li<sup>1</sup>, G. Li<sup>1</sup>, H. H. Li<sup>1</sup>, J. Li<sup>1</sup>, J. C. Li<sup>1</sup>, Q. J. Li<sup>1</sup>, R. B. Li<sup>1</sup>, R. Y. Li<sup>1</sup>, S. M. Li<sup>1</sup>, W. Li<sup>1</sup>, W. G. Li<sup>1</sup>, X. L. Li<sup>7</sup>, X. Q. Li<sup>7</sup>, X. S. Li<sup>14</sup>, Y. F. Liang<sup>13</sup>, H. B. Liao<sup>5</sup>, C. X. Liu<sup>1</sup>, Fang Liu<sup>16</sup>, F. Liu<sup>5</sup>, H. M. Liu<sup>1</sup>, J. B. Liu<sup>1</sup>, J. P. Liu<sup>17</sup>, R. G. Liu<sup>1</sup>, Y. Liu<sup>1</sup>, Z. A. Liu<sup>1</sup>, Z. X. Liu<sup>1</sup>, G. R. Lu<sup>4</sup>, F. Lu<sup>1</sup>, J. G. Lu<sup>1</sup>, C. L. Luo<sup>8</sup>, X. L. Luo<sup>1</sup>, F. C. Ma<sup>7</sup>, J. M. Ma<sup>1</sup>, L. L. Ma<sup>11</sup>, X. Y. Ma<sup>1</sup>, Z. P. Mao<sup>1</sup>, X. C. Meng<sup>1</sup>, X. H. Mo<sup>1</sup>, J. Nie<sup>1</sup>, Z. D. Nie<sup>1</sup>, S. L. Olsen<sup>15</sup>, H. P. Peng<sup>16</sup>, N. D. Qi<sup>1</sup>, C. D. Qian<sup>12</sup>, H. Qin<sup>8</sup>, J. F. Qiu<sup>1</sup>, Z. Y. Ren<sup>1</sup>, G. Rong<sup>1</sup>, L. Y. Shan<sup>1</sup>, L. Shang<sup>1</sup>, D. L. Shen<sup>1</sup>, X. Y. Shen<sup>1</sup>, H. Y. Sheng<sup>1</sup>, F. Shi<sup>1</sup>, X. Shi<sup>10</sup>, L. W. Song<sup>1</sup>, H. S. Sun<sup>1</sup>, S. S. Sun<sup>16</sup>, Y. Z. Sun<sup>1</sup>, Z. J. Sun<sup>1</sup>, X. Tang<sup>1</sup>, N. Tao<sup>16</sup>, Y. R. Tian<sup>14</sup>, G. L. Tong<sup>1</sup>, D. Y. Wang<sup>1</sup>, J. Z. Wang<sup>1</sup>, L. Wang<sup>1</sup>, L. S. Wang<sup>1</sup>, M. Wang<sup>1</sup>, Meng Wang<sup>1</sup>, P. Wang<sup>1</sup>, P. L. Wang<sup>1</sup>, S. Z. Wang<sup>1</sup>, W. F. Wang<sup>1</sup>, Y. F. Wang<sup>1</sup>, Zhe Wang<sup>1</sup>, Z. Wang<sup>1</sup>, Zheng Wang<sup>1</sup>, Z. Y. Wang<sup>1</sup>, C. L. Wei<sup>1</sup>, N. Wu<sup>1</sup>, Y. M. Wu<sup>1</sup>, X. M. Xia<sup>1</sup>, X. X. Xie<sup>1</sup>, B. Xin<sup>7</sup>, G. F. Xu<sup>1</sup>, H. Xu<sup>1</sup>, Y. Xu<sup>1</sup>, S. T. Xue<sup>1</sup>, M. L. Yan<sup>16</sup>, W. B. Yan<sup>1</sup>, F. Yang<sup>9</sup>, H. X. Yang<sup>14</sup>, J. Yang<sup>16</sup>, S. D. Yang<sup>1</sup>, Y. X. Yang<sup>3</sup>, L. H. Yi<sup>6</sup>, Z. Y. Yi<sup>1</sup>, M. Ye<sup>1</sup>, M. H. Ye<sup>2</sup>, Y. X. Ye<sup>16</sup>, C. S. Yu<sup>1</sup>, G. W. Yu<sup>1</sup>, C. Z. Yuan<sup>1</sup>, J. M. Yuan<sup>1</sup>, Y. Yuan<sup>1</sup>, Q. Yue<sup>1</sup>, S. L. Zang<sup>1</sup>, Y. Zeng<sup>6</sup>, B. X. Zhang<sup>1</sup>, B. Y. Zhang<sup>1</sup>, C. C. Zhang<sup>1</sup>, D. H. Zhang<sup>1</sup>, H. Y. Zhang<sup>1</sup>, J. Zhang<sup>1</sup>, J. M. Zhang<sup>4</sup>, J. Y. Zhang<sup>1</sup>, J. W. Zhang<sup>1</sup>, L. S. Zhang<sup>1</sup>, Q. J. Zhang<sup>1</sup>, S. Q. Zhang<sup>1</sup>, X. M. Zhang<sup>1</sup>, X. Y. Zhang<sup>11</sup>, Yiyun Zhang<sup>13</sup>, Y. J. Zhang<sup>10</sup>, Y. Y. Zhang<sup>1</sup>, Z. P. Zhang<sup>16</sup>, Z. Q. Zhang<sup>4</sup>, D. X. Zhao<sup>1</sup>, J. B. Zhao<sup>1</sup>, J. W. Zhao<sup>1</sup>, P. P. Zhao<sup>1</sup>, W. R. Zhao<sup>1</sup>, X. J. Zhao<sup>1</sup>, Y. B. Zhao<sup>1</sup>, Z. G. Zhao<sup>1\*</sup>, H. Q. Zheng<sup>10</sup>, J. P. Zheng<sup>1</sup>, L. S. Zheng<sup>1</sup>, Z. P. Zheng<sup>1</sup>, X. C. Zhong<sup>1</sup>, B. Q. Zhou<sup>1</sup>, G. M. Zhou<sup>1</sup>, L. Zhou<sup>1</sup>, N. F. Zhou<sup>1</sup>, K. J. Zhu<sup>1</sup>, Q. M. Zhu<sup>1</sup>, Yingchun Zhu<sup>1</sup>, Y. C. Zhu<sup>1</sup>, Y. S. Zhu<sup>1</sup>, Z. A. Zhu<sup>1</sup>, B. A. Zhuang<sup>1</sup>, B. S. Zou<sup>1</sup>.

(BES Collaboration)

<sup>1</sup> Institute of High Energy Physics, Beijing 100039, People's Republic of China

<sup>2</sup> China Center of Advanced Science and Technology, Beijing 100080, People's Republic of China

<sup>3</sup> Guangxi Normal University, Guilin 541004, People's Republic of China

<sup>4</sup> Henan Normal University, Xinxiang 453002, People's Republic of China

<sup>5</sup> Huazhong Normal University, Wuhan 430079, People's Republic of China

<sup>6</sup> Hunan University, Changsha 410082, People's Republic of China

<sup>7</sup> Liaoning University, Shenyang 110036, People's Republic of China

<sup>8</sup> Nanjing Normal University, Nanjing 210097, People's Republic of China

<sup>9</sup> Nankai University, Tianjin 300071, People's Republic of China

<sup>10</sup> Peking University, Beijing 100871, People's Republic of China

<sup>11</sup> Shandong University, Jinan 250100, People's Republic of China

<sup>12</sup> Shanghai Jiaotong University, Shanghai 200030, People's Republic of China

<sup>13</sup> Sichuan University, Chengdu 610064, People's Republic of China

<sup>14</sup> Tsinghua University, Beijing 100084, People's Republic of China

<sup>15</sup> University of Hawaii, Honolulu, Hawaii 96822

<sup>16</sup> University of Science and Technology of China, Hefei 230026, People's Republic of China

<sup>17</sup> Wuhan University, Wuhan 430072, People's Republic of China

<sup>18</sup> Zhejiang University, Hangzhou 310028, People's Republic of China

\* Visiting professor to University of Michigan, Ann Arbor, MI 48109 USA

ing fraction of  $J/\psi \rightarrow \pi^+\pi^-\pi^0$  is determined. The result is  $(2.10 \pm 0.12) \times 10^{-2}$ , which is significantly higher than previous measurements.

PACS numbers: 13.65.+i

## I. INTRODUCTION

Decays of the  $J/\psi$  provide an excellent source of events with which to study light hadron spectroscopy and search for glueballs, hybrids, and exotic states. Since the discovery of the  $J/\psi$  at Brookhaven [1] and SLAC [2] in 1974, more than one hundred exclusive decay modes of the  $J/\psi$  have been reported. Recently,  $5.8 \times 10^7$   $J/\psi$  events and  $1.4 \times 10^7$   $\psi(2S)$  events have been obtained with the upgraded Beijing Spectrometer (BESII), and these samples offer a unique opportunity to measure precisely the branching fractions of  $J/\psi$  decays.

The largest  $J/\psi$  decay involving hadronic resonances is  $J/\psi \rightarrow \rho(770)\pi$ . Its branching fraction has been reported by many experimental groups [3–10] assuming all  $\pi^+\pi^-\pi^0$  final states come from  $\rho(770)\pi$ . The precision of these measurements varies from 13% to 25%. In this paper, we present two independent measurements of this branching fraction using  $J/\psi$  and  $\psi(2S)$  decays. The first is an absolute measurement based on  $J/\psi \rightarrow \pi^+\pi^-\pi^0$  directly. The second, in which many of the systematic errors cancel out, is a relative measurement obtained from a comparison of the rates for  $J/\psi \rightarrow \pi^+\pi^-\pi^0$  and  $J/\psi \rightarrow \mu^+\mu^-$ , using  $J/\psi$  events produced via  $\psi(2S) \rightarrow \pi^+\pi^-J/\psi$ .

## II. THE BES DETECTOR

The upgraded BESII detector operates at the Beijing Electron-Positron Collider (BEPC); it is a large solid-angle magnetic spectrometer that is described in detail in Ref. [11]. The momentum of charged particles is determined by a 40-layer cylindrical main drift chamber (MDC) which has a momentum resolution of  $\sigma_p/p = 1.78\% \sqrt{1+p^2}$ , where  $p$  is in units of GeV/c. Particle identification is accomplished using specific ionization ( $dE/dx$ ) measurements in the drift chamber and time-of-flight (TOF) information in a barrel-like array of 48 scintillation counters. The  $dE/dx$  resolution is  $\sigma_{dE/dx} = 8.0\%$ ; the TOF resolution for Bhabha events is  $\sigma_{TOF} = 180$  ps. Radially outside the time-of-flight counters is a 12-radiation-length barrel shower counter (BSC) comprised of gas proportional tubes interleaved with lead sheets. The BSC measures the energies and directions of photons with resolutions of  $\sigma_E/E \simeq 21\% \sqrt{E(\text{GeV})}$ ,  $\sigma_\phi = 7.9$

mrad, and  $\sigma_z = 2.3$  cm. The iron flux return of the magnet is instrumented with three double layers of counters (MUC) that are used to identify muons.

In the analysis, a GEANT3 based Monte Carlo program (SIMBES) with detailed consideration of detector performance (such as dead electronic channels) is used. The consistency between data and Monte Carlo has been checked in many high purity physics channels, and the agreement is reasonable.

## III. GENERAL CRITERIA

### A. Charged Track Selection

Each charged track, reconstructed using hits in the MDC, must (1) have a good helix fit, in order to ensure a correct error matrix in the kinematic fit; (2) originate from the interaction region,  $\sqrt{V_x^2 + V_y^2} < 2$  cm and  $|V_z| < 20$  cm, where  $V_x$ ,  $V_y$ , and  $V_z$  are the x, y, and z coordinates of the point of closest approach of the track to the beam axis; (3) have a transverse momentum greater than 60 MeV/c; and (4) have  $|\cos\theta| \leq 0.8$ , where  $\theta$  is the polar angle of the track.

### B. Photon Selection

A neutral cluster in the BSC is assumed to be a photon candidate if the following requirements are satisfied: (1) the energy deposited in the BSC is greater than 0.06 GeV; (2) the total number of layers with deposited energy is greater than one; (3) the angle between the direction of photon emission and the direction of shower development is less than  $30^\circ$ ; and (4) the angle between the photon and the nearest charged track is greater than  $15^\circ$ . If the angle between two neutral clusters is less than  $10^\circ$  and their  $\gamma\gamma$  invariant mass is less than  $0.05 \text{ GeV}/c^2$ , they are combined with the cluster with the largest energy being used for the direction and energy of the combined cluster in the kinematic fit.

#### IV. ABSOLUTE MEASUREMENT OF $J/\psi \rightarrow \pi^+\pi^-\pi^0$ DECAYS

##### A. Event Selection

Events with two oppositely charged tracks and at least two good photons are selected for further analysis. No charged particle identification is required. A 5-constraint (5C) kinematic fit is made under the  $\pi^+\pi^-\gamma\gamma$  hypothesis with the invariant mass of the two photons being constrained to the  $\pi^0$  mass. If the number of the selected photons is larger than two, the fit is repeated using all permutation of the photons. For events with a good fit, the two photon combination with the minimum fit  $\chi^2_{\pi^+\pi^-\pi^0}$  is selected, and its value is required to be less than 15.

To select a clean sample, the following criteria are applied to the remaining events:

- To reject the main background events from  $J/\psi \rightarrow K^+K^-\pi^0$ , a 5C kinematic fit for  $J/\psi \rightarrow K^+K^-\pi^0$  is performed, and  $\chi^2_{\pi^+\pi^-\pi^0} < \chi^2_{K^+K^-\pi^0}$  is required. Fig. 1 shows the scatter plot of  $\chi^2_{\pi^+\pi^-\pi^0}$  versus  $\chi^2_{K^+K^-\pi^0}$ .

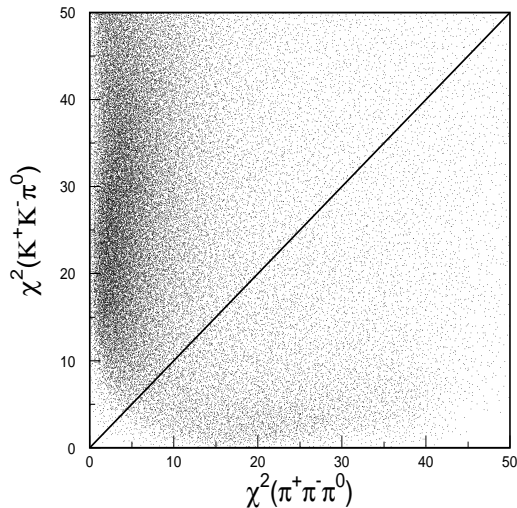


FIG. 1: Plot of  $\chi^2_{\pi^+\pi^-\pi^0}$  versus  $\chi^2_{K^+K^-\pi^0}$  for candidate  $\pi^+\pi^-\pi^0$  events. The solid line corresponds to  $\chi^2_{\pi^+\pi^-\pi^0} = \chi^2_{K^+K^-\pi^0}$ .

- Background events from  $\gamma$  conversions ( $\gamma \rightarrow e^+e^-$ ) are eliminated by requiring the angle between the two charged tracks,  $\theta_{\pi^+\pi^-}$ , to be greater than  $10^\circ$ .
- Radiative events, for example  $J/\psi \rightarrow \gamma\eta'$ , are removed by the requirement  $|\cos\theta_\gamma| < 0.98$ , where  $\theta_\gamma$  is the angle of the  $\gamma$  in the  $\pi^0$  rest frame.

- Contamination from  $J/\psi \rightarrow (\gamma)e^+e^-$  is eliminated by the requirement that the sum of the deposited energies of the two charged pions in the BSC is less than 2 GeV. Fig. 2 shows the scatter plot of  $E_{sc}^+$  versus  $E_{sc}^-$ , where  $E_{sc}^+$  and  $E_{sc}^-$  are the deposited energies of the  $\pi^+$  and  $\pi^-$  in the BSC, respectively. This criteria has almost no effect on  $\pi^+\pi^-\pi^0$  events.

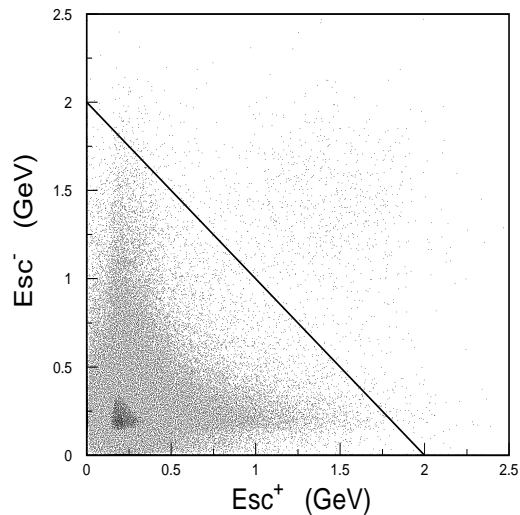


FIG. 2: Plot of  $E_{sc}^+$  versus  $E_{sc}^-$ ; the solid line is for  $E_{sc}^+ + E_{sc}^- = 2$  GeV.

After the above requirements, 219691  $\pi^+\pi^-\pi^0$  candidates are selected. Remaining backgrounds are evaluated using two different Monte Carlo simulations. In the first, specific background channels, shown in Table I, are generated. The total background from these channels in the selected  $\pi^+\pi^-\pi^0$  events is determined to be less than 1%. The second simulation uses 30 million inclusive  $J/\psi$  MC events generated with the LUND model [16]. After normalizing the selected background events to 58 million  $J/\psi$  events, 3799 background events are obtained, yielding a contamination of 1.7%. In this paper, the latter background estimate is used to correct the branching fraction, giving a correction factor of  $(98.3 \pm 1.7)\%$ .

The Dalitz plot of  $m_{\pi^+\pi^0}$  versus  $m_{\pi^-\pi^0}$  is shown in Fig. 3. Three bands are clearly visible in the plot, which correspond to  $J/\psi \rightarrow \rho^+\pi^-$ ,  $J/\psi \rightarrow \rho^0\pi^0$ , and  $J/\psi \rightarrow \rho^-\pi^+$ . The corresponding histograms of  $m_{\pi^+\pi^0}$ ,  $m_{\pi^-\pi^0}$ , and  $m_{\pi^+\pi^-}$  are shown in Fig. 4. From the Dalitz plot (Fig. 3), we see that  $J/\psi \rightarrow \pi^+\pi^-\pi^0$  is strongly dominated by  $\rho\pi$ . Therefore, the detection efficiency is determined using the RHOPI [17] generator with SIMBES and is found to be 17.83%. Monte Carlo simulation using other generators to represent the structure in the Dalitz plot, provide very similar

TABLE I: Background contributions from different decay channels. Here  $N_{bkg}$  is the number of events generated, and  $N_{bkg}^{norm}$  is the number of background events selected, normalized by the branching fractions quoted in Ref. [15].

Decay Channel	$N_{bkg}$	$N_{bkg}^{norm}$
$J/\psi \rightarrow K^{*+}K^{-} + c.c. (K^{+}K^{-}\pi^{0})$	100,000	773
$J/\psi \rightarrow K^{*+}K^{-} + c.c. (KK_{S}^{0}\pi)$	50,000	153
$J/\psi \rightarrow K^{*0}\bar{K}^{0} + c.c. (KK_{S}^{0}\pi)$	50,000	129
$J/\psi \rightarrow \gamma\eta' (\gamma\gamma\rho)$	100,000	158

detection efficiencies.

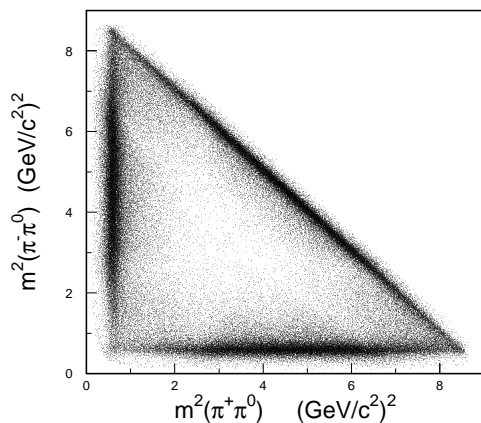


FIG. 3: The Dalitz plot for  $J/\psi \rightarrow \pi^{+}\pi^{-}\pi^{0}$ .

## B. Systematic Error Analysis

In this analysis, the systematic error on the branching fraction comes mainly from the following sources:

- MDC tracking

The MDC tracking efficiency has been measured using channels like  $e^{+}e^{-} \rightarrow (\gamma)e^{+}e^{-}$ ,  $e^{+}e^{-} \rightarrow (\gamma)\mu^{+}\mu^{-}$ ,  $J/\psi \rightarrow \Lambda\bar{\Lambda}$ , and  $\psi(2S) \rightarrow \pi^{+}\pi^{-}J/\psi$ ,  $J/\psi \rightarrow \mu^{+}\mu^{-}$ . It is found that the Monte Carlo simulation agrees with data within 1-2% for each charged track. The systematic error on the tracking efficiency for the channel of interest is taken as 4%.

- Photon detection efficiency

The photon detection efficiency is studied with  $J/\psi \rightarrow \rho^{0}\pi^{0}$  events. Events with two oppositely charged tracks and at least one photon are selected. The two charged tracks are required to

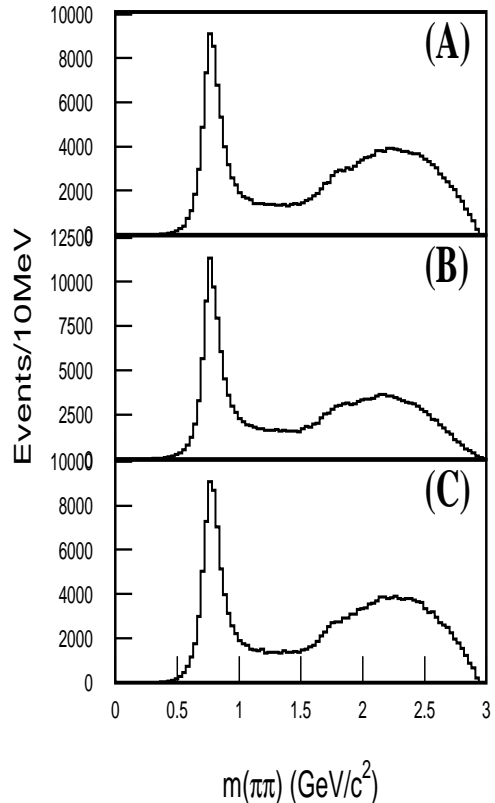


FIG. 4: The distributions of invariant mass of two pions for (A)  $m_{\pi^{+}\pi^{0}}$ , (B)  $m_{\pi^{+}\pi^{-}}$ , and (C)  $m_{\pi^{-}\pi^{0}}$ .

be identified as pions using particle identification. A 2C kinematic fit is made under the hypothesis  $\pi^{+}\pi^{-}\gamma\gamma_{missing}$ , where  $\gamma_{missing}$  is a missing photon and the  $\gamma\gamma_{missing}$  invariant mass is constrained to the  $\pi^{0}$  mass. The combination with the smallest  $\chi^2$  is selected and is required to satisfy  $\chi^2 < 10$ , as well as be less than the  $\chi^2$  of the 2C kinematic fit with the two charged tracks assumed to be kaons. Events with  $0.62 \text{ GeV}/c^2 < m_{\pi^{+}\pi^{-}} < 0.92 \text{ GeV}/c^2$ ,  $m_{\pi^{-}\pi^{0}} > 1.2 \text{ GeV}/c^2$ , and  $m_{\pi^{+}\pi^{0}} > 1.2 \text{ GeV}/c^2$  are selected as  $\rho^0$  candidates. The “missing” photon’s energy distribution is large enough to cover the case of  $\rho^{\pm}\pi^{\mp}$ , so it is used to study the photon detection efficiency. The same analysis is performed with Monte Carlo events. The gamma detection efficiency for data is in good agreement with that from Monte Carlo. The difference between them is about 2% for each photon which is taken as the systematic error.

- Kinematic fit and other criteria

To estimate the systematic error from the 5C kinematic fit, we select a clean  $\rho\pi$  sample with-

out the kinematic fit. Events with two oppositely charged tracks and two good photons are selected. The charged tracks must be identified as pions. The direction of  $\mathbf{P}_{\text{miss}}$ , where  $\mathbf{P}_{\text{miss}}$  is the missing momentum determined using the charged tracks, is regarded as the direction of the  $\pi^0$  and used to calculate the invariant mass of the two photons, which is required to be less than  $0.2 \text{ GeV}/c^2$ . A variable  $U_{\text{miss}} = E_{\text{miss}} - |\mathbf{P}_{\text{miss}}|$  is defined, where  $E_{\text{miss}}$  is the missing energy of the two charged tracks which is calculated assuming the charged tracks are pions.  $U_{\text{miss}}$  is required to be less than zero to select a clean sample.

A 5C kinematic fit is done on the candidates. The same analysis is also performed with Monte Carlo events. By comparing the number of events with and without a good 5C kinematic fit, the efficiencies for  $\chi^2_{\pi^+\pi^-\pi^0} < 15$  are measured to be 76.5% and 79.8% for real data and Monte Carlo simulation, respectively. The difference between them is 4.1% and a correction factor, 1.041, is obtained, and the systematic error on this correction is taken as 4.1%.

To estimate the systematic error from the  $\chi^2_{\pi^+\pi^-\pi^0} < \chi^2_{K^+K^-\pi^0}$  requirement, we selected events where both charged tracks are identified as pions using particle identification. The branching fraction is then obtained with all the selection criteria described above. The difference between this result and that calculated without the  $\chi^2_{\pi^+\pi^-\pi^0} < \chi^2_{K^+K^-\pi^0}$  requirement is regarded as the systematic error caused by this criteria. In fact, the difference between them is very small, and the error caused by this criteria is less than 1%.

For the requirements  $\theta_{\pi^+\pi^-} > 10^\circ$  and  $|\cos\theta_\gamma| < 0.98$ , just a few events are excluded by these selection criteria; the systematic error for them can be ignored. From the scatter plot shown in Fig. 2, the requirement on the deposited energy of two charged pions has almost no effect on the  $\pi^+\pi^-\pi^0$  candidates, so the systematic error from this selection criteria is also neglected. The total systematic error from the kinematic fit and other criteria discussed in this section is 4.2%, which is the sum of these errors added in quadrature.

- Uncertainty of the hadronic model

Different simulation models for the hadronic interaction give different efficiencies, leading to

different branching fractions. In this analysis, two models, FLUKA [12] and GCALOR [13], are used in the simulation of hadronic interactions in SIMBES. The difference between the detection efficiencies from them is about 1.7%, which is regarded as the systematic error.

- Uncertainty of background

Above we estimated backgrounds for several possible decay channels. Given the uncertainties of the branching fractions of background channels and possible unknown decay modes of  $J/\psi$ , we estimate the uncertainty of the background is less than 3%.

The contributions from all sources are listed in Table II. The systematic errors caused by Monte Carlo statistics and the error in the number of  $J/\psi$  events are also listed. The total systematic error in Table II is the sum of them added in quadrature.

TABLE II: Summary of correction factors  $f_c$  and systematic errors

Sources	$f_c$	Systematic error (%)
MDC tracking		4
Photon efficiency		4
Kinematic fit	1.041	4.2
Hadronic model		$\sim 3$
Backgrounds	0.983	1.7
MC statistics		0.4
Number of $J/\psi$ events		4.7
Total	1.023	9.2

### C. Branching Fraction of $J/\psi \rightarrow \pi^+\pi^-\pi^0$

For the decay of  $J/\psi \rightarrow \pi^+\pi^-\pi^0$ , the branching fraction is obtained with the following formula

$$Br(J/\psi \rightarrow \pi^+\pi^-\pi^0) = \frac{N_{\pi^+\pi^-\pi^0}^{\text{obs}}}{N_{J/\psi} \cdot \epsilon} \cdot f_c \quad (1)$$

where  $N_{\pi^+\pi^-\pi^0}^{\text{obs}}$  is the observed number of  $\pi^+\pi^-\pi^0$  events,  $\epsilon$  is the detection efficiency obtained from the MC simulation,  $N_{J/\psi}$  is the total number of  $J/\psi$  events,  $(57.7 \pm 2.7) \times 10^6$ , which is determined from the number of inclusive 4-prong hadrons [14]; and  $f_c$  is the kinematic fit and background contamination correction factor.

With the above formula, the branching fraction of  $J/\psi \rightarrow \pi^+\pi^-\pi^0$  is

$$Br(J/\psi \rightarrow \pi^+\pi^-\pi^0) = (21.84 \pm 0.05 \pm 2.01) \times 10^{-3}$$

where the first error is statistical and the second systematic.

## V. RELATIVE MEASUREMENT OF

$$J/\psi \rightarrow \pi^+\pi^-\pi^0$$

The relative measurement is based on a sample of 14 million  $\psi(2S)$  events. The  $\psi(2S)$  is a copious source of  $J/\psi$  decays: the branching fraction of  $\psi(2S) \rightarrow \pi^+\pi^-J/\psi$  is the largest single  $\psi(2S)$  decay channel. Therefore, we can determine the branching fraction of  $J/\psi \rightarrow \pi^+\pi^-\pi^0$  from a comparison of the following two processes:

$$\begin{aligned} \psi(2S) \rightarrow \pi^+\pi^- J/\psi & \\ \hookrightarrow \pi^+\pi^-\pi^0 & \quad (I) \\ \text{and } \psi(2S) \rightarrow \mu^+\mu^- & \quad (II) \end{aligned}$$

The branching fraction is determined from the relation:

$$B(J/\psi \rightarrow \pi^+\pi^-\pi^0) = \frac{N_I^{obs}}{N_{II}^{obs}} \cdot \frac{\epsilon_{II}}{\epsilon_I} \cdot B(J/\psi \rightarrow \mu^+\mu^-), \quad (2)$$

where  $N_I^{obs}$  and  $N_{II}^{obs}$  are the observed numbers of events for processes I and II, and  $\epsilon_I$  and  $\epsilon_{II}$  are the respective acceptances. The branching fraction for the leptonic decay  $J/\psi \rightarrow \mu^+\mu^-$ ,  $B(J/\psi \rightarrow \mu^+\mu^-) = (5.88 \pm 0.10)\%$ , is obtained from the Particle Data Group (PDG) [15]. Using the relative measurement, many systematic errors, for instance, the errors of the total number of  $\psi(2S)$  events, the branching fractions of  $\psi(2S) \rightarrow \pi^+\pi^-J/\psi$ , and the efficiency for  $\psi(2S) \rightarrow \pi^+\pi^-J/\psi$ , etc, mostly cancel. Therefore, the precision of the branching fraction  $J/\psi \rightarrow \pi^+\pi^-\pi^0$  from the relative measurement is comparable with that of the direct  $J/\psi$  decay, as we will see later, although the size of  $\psi(2S)$  sample is smaller than the  $J/\psi$  sample.

### A. Event Selection

Candidate events for  $\psi(2S) \rightarrow \pi^+\pi^-J/\psi$ ,  $J/\psi \rightarrow \mu^+\mu^-$  or  $\pi^+\pi^-\pi^0$  are required to have four charged tracks with total charge zero. Each track is required to satisfy the general criteria described in Section III. For both processes I and II, we require at least one pair of oppositely charged candidate pion tracks that each satisfy the following criteria:

- $p_\pi < 0.5$  GeV/c, where  $p_\pi$  is the pion momentum.
- $\cos\theta_{\pi\pi} < 0.9$ , where  $\theta_{\pi\pi}$  is the laboratory angle between the  $\pi^+$  and  $\pi^-$ . This requirement is

used to eliminate contamination from misidentified  $e^+e^-$  pairs from  $\gamma$  conversions.

The invariant mass recoiling against the candidate  $\pi^+\pi^-$  pair,  $m_{recoil}^{\pi^+\pi^-} = [(m_{\psi(2S)} - E_{\pi^+} - E_{\pi^-})^2 - (p_{\pi^+} + p_{\pi^-})^2]^{1/2}$ , is required to be in the range  $3.0 \leq m_{recoil}^{\pi^+\pi^-} \leq 3.2$  GeV/c<sup>2</sup>.

For process I, candidate events are required to satisfy the following additional criteria:

- All four charged tracks are assumed to be  $\pi^\pm$  directly, and no particle identification is required.
- The number of photon candidates must be equal to or greater than two.
- A 5C kinematic fit is performed for each  $\psi(2S) \rightarrow \pi^+\pi^-\pi^+\pi^-\pi^0$  candidate event, and the event probability given by the fit must be greater than 0.01 and greater than that of  $\psi(2S) \rightarrow \pi^+\pi^-K^+K^-\pi^0$ .
- Remaining background from  $J/\psi$  to  $e^+e^-$  and  $\mu^+\mu^-$  events is removed with the following requirement:  $[(\chi_e^+ + \chi_e^-)^2/9 + (E_{sc}^+ + E_{sc}^- + \mu_{id}^+ + \mu_{id}^- - 2.5)^2/3] > 1$  and  $E_{sc}^+ + E_{sc}^- + \mu_{id}^+ + \mu_{id}^- < 6$ , as shown in Fig. 5. Here  $\chi_e$  is the difference between the  $dE/dx$  measured with the MDC and that expected for the electron hypothesis divided by the  $dE/dx$  resolution,  $E_{sc}$  is the energy deposited in the BSC, and  $\mu_{id}$  is the number of MUC layers with matched hits and ranges from 0 to 3. The contamination from  $J/\psi \rightarrow e^+e^-$  or  $\mu^+\mu^-$  is estimated to be 0.4% from Monte Carlo simulation.

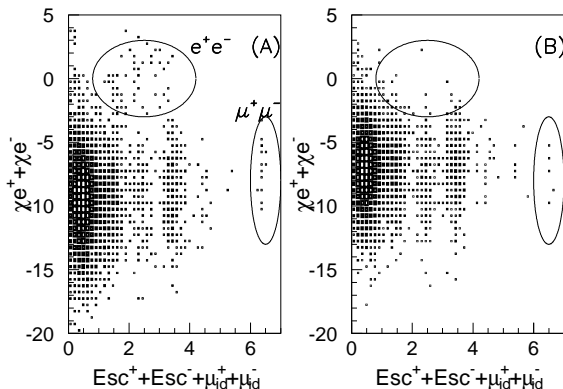


FIG. 5: Scatter plots of  $\chi_{e^+} + \chi_{e^-}$  versus  $E_{sc}^+ + E_{sc}^- + \mu_{id}^+ + \mu_{id}^-$  for (a.) data and (b.) MC.

The Dalitz plot of candidate  $J/\psi \rightarrow \pi^+\pi^-\pi^0$  events is shown in Fig. 6. The contamination from  $J/\psi \rightarrow K^*K$  is about 1.0% and is estimated from Monte

Carlo simulation. Those of other backgrounds (e.g.  $e^+e^-$ ,  $\mu^+\mu^-$ , and  $\gamma\gamma\rho$ ) are much less than 1.0%.

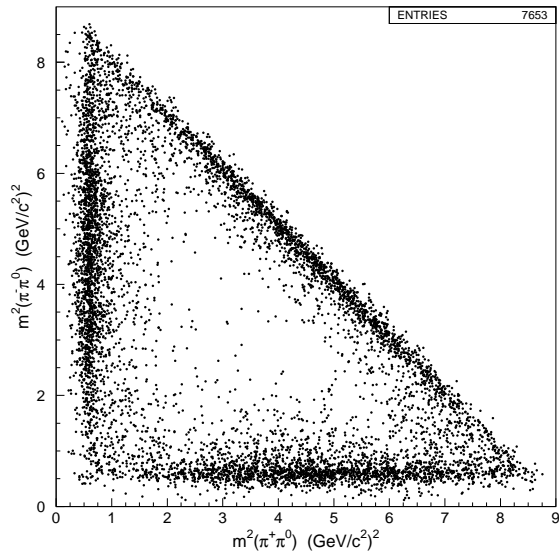


FIG. 6: Dalitz plot for candidate  $J/\psi \rightarrow \pi^+\pi^-\pi^0$  events. Here the  $J/\psi$  comes from  $\psi(2S) \rightarrow \pi^+\pi^-J/\psi$  decay.

To reduce possible systematic bias caused by inconsistencies between data and Monte Carlo, similar requirements are used for  $J/\psi \rightarrow \mu^+\mu^-$  candidate events (process II).

- The two higher momentum tracks are assumed to be  $\mu^\pm$ , and no muon identification is required.
- A 4C kinematic fit is performed for  $\psi(2S) \rightarrow \pi^+\pi^-\mu^+\mu^-$  candidate events, and the probability given by the fit must be greater than 0.01.
- The contamination from  $J/\psi \rightarrow e^+e^-$  is removed with the requirement  $E_{sc}^\pm < 0.8$  GeV. After this, the contamination from  $e^+e^-$  is less than 0.8%, estimated from Fig. 7a, and  $\sim 0.4\%$  from MC simulation.

Fig. 7b shows the scatter plot of  $m_{recoil}^{\pi^+\pi^-}$  versus  $m_{\mu^+\mu^-}$  for  $\psi(2S) \rightarrow \pi^+\pi^-J/\psi \rightarrow \pi^+\pi^-\mu^+\mu^-$  candidate events. MC simulations of  $J/\psi$  decays to  $\pi^+\pi^-$ ,  $K^+K^-$ ,  $p\bar{p}$  and  $\rho\pi$  indicate that background from these processes can be ignored.

By fitting the invariant mass recoiling against the  $\pi^+\pi^-$  pair in  $\psi(2S) \rightarrow \pi^+\pi^-J/\psi$ ,  $J/\psi \rightarrow \mu^+\mu^-$  decay, one obtains the  $m_{recoil}^{\pi^+\pi^-}$  spectrum, which is then used to fit the recoil mass spectrum of the  $\psi(2S) \rightarrow \pi^+\pi^-J/\psi$ ,  $J/\psi \rightarrow \pi^+\pi^-\pi^0$  process, as shown in Fig 8. We obtain  $\frac{N_I^{obs}}{N_{II}^{obs}} = 0.102 \pm 0.001$  and use the same procedure on simulated data to determine  $\frac{\epsilon_I}{\epsilon_{II}} = 0.286 \pm 0.003$ , so the ratio of  $B(J/\psi \rightarrow$

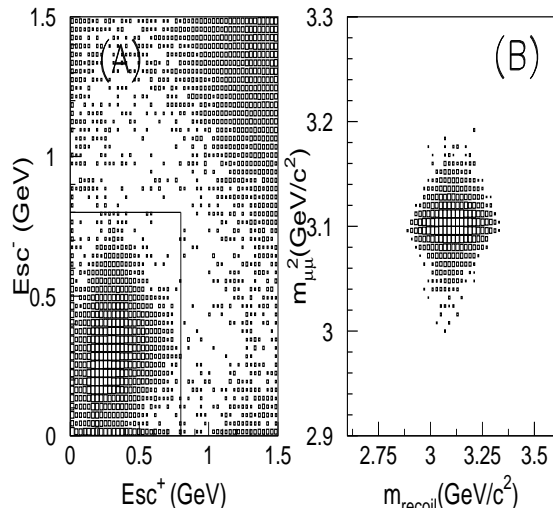


FIG. 7: (a) Deposited energy in BSC for  $\mu^+$  and  $\mu^-$  and (b.) plot of  $m_{recoil}^{\pi^+\pi^-}$  versus  $m_{\mu^+\mu^-}$  for candidate  $\psi(2S) \rightarrow \pi^+\pi^-J/\psi$ ,  $J/\psi \rightarrow \mu^+\mu^-$  events.

$\pi^+\pi^-\pi^0$ ) to  $B(J/\psi \rightarrow \mu^+\mu^-)$  is  $(35.7 \pm 0.5)\%$ . Here the errors are the statistical uncertainties combined with the uncertainties in the fitting procedure.

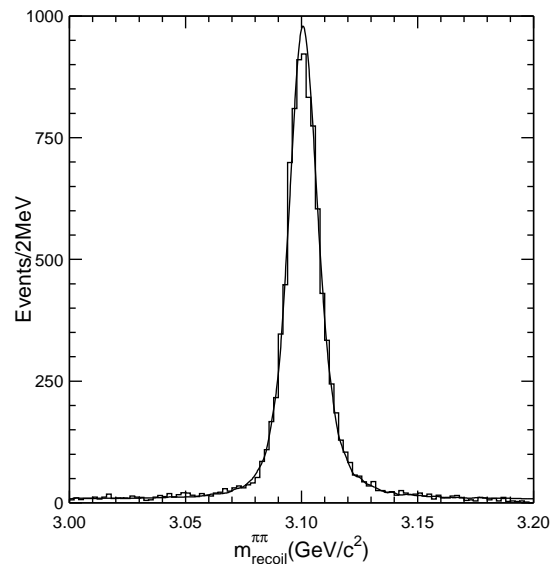


FIG. 8: Fitting the  $\pi^+\pi^-$  recoil mass of  $\psi(2S) \rightarrow \pi^+\pi^-J/\psi$ ,  $J/\psi \rightarrow \rho\pi$  (the histogram) with the  $m_{recoil}^{\pi^+\pi^-}$  spectrum parameters obtained from  $\psi(2S) \rightarrow \pi^+\pi^-J/\psi$ ,  $J/\psi \rightarrow \mu^+\mu^-$  (the curve).

## B. Systematic Error Analysis

Systematic errors come from background uncertainties, the uncertainties of  $B(J/\psi \rightarrow \mu^+\mu^-)$  and  $B(\pi^0 \rightarrow \gamma\gamma)$ , and imperfections in the Monte Carlo

simulations.

Since similar requirements are used for processes I and II, many systematic errors cancel out. For instance, the uncertainty in the selection of the  $\pi^+\pi^-$  pair recoiling against the  $J/\psi$  will not contribute to the systematic error. Other uncertainties are treated in the following:

- MDC tracking

This systematic error is caused by differences between MDC tracking efficiencies for data and Monte Carlo simulation. Since the Monte Carlo simulation agrees with data within 1 to 2% for each charged track, this systematic error is less than 2.0%.

- Photon detection efficiency

Two photons are involved in process I and no photons in process II. The uncertainty of photon selection is about 4% according to the study described in Section IV B.

- Uncertainty of the Hadronic model

Since  $J/\psi \rightarrow \pi^+\pi^-\pi^0$  is strongly dominated by the  $\rho(770)\pi$  dynamics and the contribution of the excited rho states is still unknown, a  $\psi(2S) \rightarrow \pi^+\pi^-J/\psi$ ,  $J/\psi \rightarrow \rho\pi$  simulation is used to obtain the detection efficiency ( $\epsilon_I$ ). The effect of the excited rho states is estimated to be about 1.0%.

The difference found from different models of the hadronic interaction (GCOLAR and FLUKA) is 1.2%.

- Kinematic fit

A kinematic fit is performed for both processes I and II, and the probability given by the fit is required to be greater than 0.01. Since the kinematic fit depends on the error matrix from track fitting, a systematic error of 1.5% is estimated from the difference of the error matrix for data and Monte Carlo simulation. In addition,  $\chi^2(\pi^+\pi^-\pi^+\pi^-\pi^0) < \chi^2(\pi^+\pi^-K^+K^-\pi^0)$  is used for process I, which causes a correction factor of  $(1.2 \pm 0.5)\%$ , determined from an analysis similar to that described in Section IV B.

- Uncertainty of background

Above we estimated possible backgrounds for processes I and II, and contaminations of about 2.0% and 0.4% were obtained, respectively. We have also used a sample of 14 million inclusive  $\psi(2S)$  MC events generated with the LUND

model [16] to estimate the contribution of background for process I, and the contamination is found to be less than 3.0%; a background correction factor  $(98.4 \pm 1.5)\%$  is used.

Other requirements, such as those to remove  $J/\psi \rightarrow e^+e^-$  or  $\mu^+\mu^-$  for process I and to remove  $J/\psi \rightarrow e^+e^-$  for process II, have very high efficiencies ( $\sim 100\%$ ). Their systematic error contributions are ignored.

Table III summarizes all systematic errors. The largest comes from the uncertainty of the photon efficiency. The table also includes correction factors from the kinematic fit and background contamination.

TABLE III: Summary of correction factors  $f_c$  and systematic errors (%).

	$f_c$	Sys. err. (%)
MDC tracking		2.0
Kinematic fit	1.012	1.6
Photon efficiency		4.0
Backgrounds	0.984	1.6
Hadronic model		1.6
$B(J/\psi \rightarrow \mu^+\mu^-)$		1.7
$B(\pi^0 \rightarrow \gamma\gamma)$		0.03
MC statistics		1.0
Total	0.996	5.6

### C. Branching fraction

The branching fraction calculated with formula (2) multiplied by the correction factor  $f_c$  is

$$B(J/\psi \rightarrow \pi^+\pi^-\pi^0) = (20.91 \pm 0.21 \pm 1.16) \times 10^{-3}.$$

## VI. FINAL RESULT AND DISCUSSION

The absolute branching fraction of  $J/\psi \rightarrow \pi^+\pi^-\pi^0$  has been determined using a sample of 58 million  $J/\psi$  decays, as well as by measuring the relative branching fraction of  $J/\psi \rightarrow \pi^+\pi^-\pi^0$  to  $J/\psi \rightarrow \mu^+\mu^-$  in  $\psi(2S) \rightarrow \pi^+\pi^-J/\psi$  decays with a sample of 14 million  $\psi(2S)$  events. The results are in good agreement. The weighted mean of these two measurements is

$$B(J/\psi \rightarrow \pi^+\pi^-\pi^0) = (2.10 \pm 0.12)\%.$$

The only reported branching fraction for  $J/\psi \rightarrow \pi^+\pi^-\pi^0$  is by Mark-II [8], whereas many experiments have reported measurements for  $J/\psi \rightarrow \rho\pi$  [3–7, 9, 10], which contributes the dominant part of the



$\pi^+\pi^-\pi^0$  final state. The result obtained here is higher than those of previous measurements and has better precision.

### Acknowledgments

The BES collaboration thanks the staff of BEPC for their hard efforts. This work is supported in part by the National Natural Science Foundation of China under contracts Nos. 19991480, 10225524, 10225525, the Chinese Academy of Sciences under contract No. KJ

95T-03, the 100 Talents Program of CAS under Contract Nos. U-11, U-24, U-25, and the Knowledge Innovation Project of CAS under Contract Nos. U-602, U-34(IHEP); by the National Natural Science Foundation of China under Contract No. 10175060 (USTC); and by the Department of Energy under Contract No. DE-FG03-94ER40833 (U Hawaii).

- 
- [1] J. J. Aubert et al., Phys. Rev. Lett. **33**, 1404 (1974).  
 [2] J. E. Augustin et al., Phys. Rev. Lett. **33**, 1406 (1974).  
 [3] B. Jean-Marie et al., Phys. Rev. Lett. **36**, 291 (1976).  
 [4] W. Braunschweig et al., Phys. Lett. **63B**, 487 (1976).  
 [5] W. Bartel et al., Phys. Lett. **64B**, 483 (1976).  
 [6] G. Alexander et al., Phys. Lett. **72B**, 493 (1978).  
 [7] R. Brandelik et al., Phys. Lett. **74B**, 292 (1978).  
 [8] M. E. B. Franklin et al., Phys. Rev. Lett. **51**, 963 (1983).  
 [9] D. Coffman et al., Phys. Rev. **D38**, 2695 (1988).  
 [10] J. Z. Bai et al., Phys. Rev. **D54**, 1221 (1996).  
 [11] J. Z. Bai et al., Nucl. Instrum. Methods Phys. Res. Sec. **A458**, 627 (2001).  
 [12] K. Hanssger, H. J. Mohring and J. Ranft, Nucl. Sci. Eng. 88 (1984), 551; J. Ranft and S. Ritter, Z. Phys. C20 (1983), 347. A. Fasso et al., FLUKA 92, Proceedings of the Workshop on Simulating Accelerator Radiation Environments, Santa Fe, 1993.  
 [13] C. Zeitnitz and T. A. Gabriel, NIM A349 (1994) 106-111.  
 [14] S. S. Fang et al., HEP&NP, 27 (4), 277 (2003) (in Chinese).  
 [15] Particle Data Group, K. Hagiwara et al., Phys. Rev. **D66**, 010001 (2002), and references therein.  
 [16] J. C. Chen et al., Phys. Rev. **D62**, 034003 (2000).  
 [17] Generator for generating  $\rho\pi$  events with the angular distribution of  $J/\psi$  decays into pseudoscalar plus vector mesons. The angular distribution is described by  $\frac{d^3\sigma}{d\cos\theta_V d\cos\theta_1 d\phi_1} = \sin^2\theta_1 [1 + \cos^2\theta_V + \sin^2\theta_V \cos(2\phi_1)]$  where  $\theta_V$  is the angle between the vector meson and the positron direction. For  $\rho \rightarrow \pi\pi$ ,  $\theta_1$  and  $\phi_1$  are the polar and azimuthal angles of the  $\pi$  with respect to the helicity direction of the  $\rho$ .